Wetting phenomena observed in evaporating droplets on structured surfaces

Wetting phenomena observed in evaporating droplets on structured surfaces

Revekka Tekidou, Gail Duursma* , Coinneach Mackenzie-Dover , Veronika Kubyshkina,

Jonathan Terry, Khellil Sefiane

School of Engineering, The University of Edinburgh, Kings Buildings, Mayfield Road, Edinburgh EH9 3JL, UK

*Address correspondence to Dr Gail Duursma, School of Engineering, The University of Edinburgh, The King's Buildings, Mayfield Road, Edinburgh EH9 3JL, UK E-mail: gail.duursma@ed.ac.uk

Phone Number: 0 (+44) 131 650 4868, Fax Number: 0 (+44) 131 650 6551

ABSTRACT

A study was undertaken of ethanol droplet evaporation on structured surfaces of pillars (square pillars of variable dimensions and spacing of order microns, and cylindrical of various spacings). On seasoned perflourodecyltrichlorosilane surfaces, significant films were observed extending far beyond the initial contact line for pure ethanol droplets, most prominently for 4 microlitre droplets. On parylene coated surfaces, similar imbibed films were seen for 1.5 microlitre droplets of 50% by volume ethanol-water mixture. This film acts as an additional surface for evaporation and it appears that the droplet then serves as a reservoir for feeding the film until the evaporation process is completed, rather than evaporation being governed by evaporation at the contact line. The droplets with films show higher evaporation rates.

INTRODUCTION

Droplets on microstructured surfaces are of major significance in the area of microscale heat transfer with special reference to microelectronics cooling, Fukutani *et al.* [1], Duursma *et al.* [2], and Mackenzie-Dover *et al.* [3]. The behaviour on flat substrates (see e.g. Sefiane *et al*. [4], Wasnik *et al*. [5], Tadmor *et al*. [6]) has been studied though the full mechanism of droplet evaporation remains elusive.

Droplets of low volatility fluids on hydrophobic structured surfaces adopt the Cassie-Baxter configuration of "fakir" droplets above the peaks of the structure and air fills the voids in the structure. The Wenzel state by contrast is a fully wetted state with no air underneath the droplet.

It has also been reported that geometrical droplets can be formed using particular fluids on such structured surfaces, Papadopoulos *et al.* [7]. Some surface configurations allow spreading and indeed directed spreading can be induced with certain surface structure choices (Chu *et al.* [8]). Polygonal spreading of droplets which remain mostly circular has been shown by Courbin *et al*. [9, 10], though the surfaces and fluids used largely differ from those in this work. Courbin *et al.* report a spreading front, l, dependence on time, t:

$$l \sim \sqrt{t} \qquad (1)$$

The spreading dynamics were obtained using water. In two-dimensional spreading, a wicking diffusivity has also been obtained akin to Darcy flow in a porous medium and this also allows the spreading front to depend on the square root of t. Diffusivities of surfaces are a function of pillar spacing (but cylindrical pillars were used for the substrate). The dynamics of spreading is also discussed in a review by Bonn *et al.* [11].

Hu and Larson [12] obtained the evaporative flux for a pinned droplet (see Tadmor *et al*. [13], Tadmor [14] on a flat substrate from a computational model and showed that the evaporation occurred mainly at the contact line on a flat surface.

Feng *et al.* [15] used a micropyramidal substrate and ethanol-water mixtures up to a concentration of 30%. They observe initially pinned geometrical drops (octagonal) which subsequently shrink.

Very recent work (Zhong *et al.* [16]) involved the addition of surfactants to control wetting geometry.

It is known that evaporation facilitates the rapid transition from the Cassie-Baxter to the Wenzel state as described by Tsai *et al.* [17] who used water droplets in their study, whereas more volatile fluids are used in this work.

In this study, coated silicon surfaces with square or cylindrical pillars are used to create geometrical droplets and to study film spreading by imbibition from some of these droplets. The pillar spacings used in this work are rather closer than those used by other researchers, for example Courbin *et al*. [10]. The fluid used is pure ethanol for the work with perflourodecyltrichlorosilane (FDTS) coating which means that evaporation is rapid and confounds the fluid dynamics of spreading and imbibition into the forest of pillars. A 50% water-ethanol mixture was used on parylene coated surfaces, in order to create similarly formed droplets with films, and evaporation rates were studied for these surfaces as well.

EXPERIMENTAL

Microstructured surfaces, as seen in Figure 1, were manufactured at the Scottish Microelectronics Centre at the University of Edinburgh. The surfaces are 1 × 1 cm^2 arrays of uniformly sized and spaced micropillars. Arrays of square micropillars of different lateral dimensions (for example 5 × 5, 10 × 10, 20 × 20 μm^2) are spaced from their adjacent neighbours by 5, 10, 20, 40, 80 and 160 μm. The surfaces were fabricated via photolithography and reactive-ion etching techniques on silicon wafers (SI-MAT). These wafers were coated in FDTS and later new wafers were coated in parylene. Cylindrical pillars of 10 microns were also used at three spacings of 5, 10 and 20 microns.

Ethanol (C_2H_5OH) droplets evaporating on these surfaces were regarded from two perspectives simultaneously. A CCD camera was mounted at a small angle to the normal of the surface to register a pseudo-bird's-eye view of the surface and monitor the overall shape and spreading of the droplet. A second camera, which formed part of the Drop-Shape Analyser (DSA30, Kruss) goniometer, observed the evaporating ethanol droplet while the angle between the droplet edge and the surface. A labelled photograph of the experimental setup is displayed in Figure 1. Examination of ethanol droplets of 1 and 4 microlitres was carried out.

On the parylene surfaces, water showed hydrophobic behaviour and pure ethanol wet the surface completely, showing omniphilic behaviour. Droplets of a 50% water-ethanol mixture of volume 1.5 μl were used as these showed similar films spreading to the ethanol droplets on the FDTS coated surfaces.

Surfaces were cleaned between runs. This was done by a procedure of rinsing and immersion in an ultrasound bath.

RESULTS AND DISCUSSION

On these structured surfaces, droplet shapes on deposition assume an interesting geometry, as shown in Figure 2 for square pillars of two sizes and four spacings on FDTS coated silicon. Some droplets are seen to be pseudo-octagonal whereas some with larger pillars and spacings are almost spherical.

A phenomenological study of evaporation of these droplets (and films) was next undertaken and the images extracted from the videos are seen in Figure 3 for various morphologies. For the smallest pillars and spacing (Figure 3(a-c)), the film is shown at its full extent at 27 s and it remains at this size for a duration during which there is apparent evaporation from the droplet and film until the droplet appears to have been dissipated and the full film evaporates until all fluid has changed phase.

In Figure 3(d-f), the 5 micron pillars are at a spacing of 10 microns and here the film spreads again but after reaching its full extent, film evaporation leads to a retraction of the corner of the square film, whereas the droplet remains identifiable at the centre of the film even at 105 s.

For the 10 micron pillars at 5 micron spacing (Figure 3(g-i)), there is more pronounced evaporation from the film corners. The evaporation progresses rapidly once it has has begun at about 80 s.

For 10 micron pillars at a spacing of 10 microns (Figure 3(j-l)), the droplet-film interface is seen to retreat towards the centre and the film is maintained until about 50 seconds, whereafter film evaporation is evident, with retreating film edges clearly seen.

In Figure 4, the final evaporation stage of a 1 microlitre droplet is seen to show that evaporation in this period of the droplet lifetime takes place across the full area of the film. In Figure 5, the 4 microlitre droplet spreading stage (two seconds) is shown, revealing the mechanism of spread by engulfing a pillar at the far end of a row and filling in around each successive pillar in that row. Also evident is that the final phase of evaporation occurs near the centre with the film edges evaporated well before the end of the droplet lifetime.

In Figure 6, the volume of two drops, one with a film and one without, are plotted. (Optical techniques for volume determination assume axisymmetry, which is broached for geometrical drops and volume for these is therefore approximate). The surfaces are 10 micron cylindrical pillars and two spacings (5 and 20 microns) were chosen as this gave one droplet with a film and one without. It is hard to estimate at each timestep the proportion of water and ethanol evaporated however it is possible to do an integral balance to estimate the mass rate and corresponding enthalpy rate. Enthalpy rates are shown in the figure and tabulated in Table 1. The evaporation rate is clearly larger for the droplet with a film. The evaporation timescale for a droplet with base (excluding film area) of 2 mm is 140 seconds, which could be compared with droplets without films e.g. Sefiane *et al.* [4], where evaporation rates for a same base size droplet (and roughly comparable volume) are about 200 seconds. This implies that evaporation is not just confined to the contact line as per the model of Hu and Larson [12], but that film evaporation plays a significant role. For droplets with films, the reservoir feeding the imbibition between pillars which leads to film formation is shown schematically in the inset in Figure 6. Evaporation rate is relatively constant implying a persistent film, or a pinned drop for the case where the film is negligible.

This also implies that the imbibition must be sufficient to at least balance film evaporation. Capillary forces (see Tadmor *et al.* [18], N'guessan *et al.* [19]) drive the imbibition but viscous forces retard it and these will be greater for shallower films. We postulate that the pillars act to promote imbibition of fluid through the morphology replenishing the ethanol from the droplet which acts as a reservoir for the film evaporation, not just as an evaporating surface itself. In many of these instances, the film persists until the end of the evaporation of all the fluid and there is no last phase with just the droplet evaporating – i.e. the droplet acts as the film reservoir until the last stages of the process.

For the most circular of droplets, the evaporation (as given by droplet height vs time) is shown in Figure 7 for three morphologies. This plot is seen to be near-linear, with largest film giving highest rate but there is not a clear trend by film area. If the imbibition is proportional to the square root of time, and the area to the square of lengthscale, this would suggest that the evaporation rate (for short timescales when spreading occurs) would be constant if the film area all contributed equally to the evaporative flux, without the extra evaporative flux from the contact line. In these cases the much greater extent of the film and the need for the liquid to travel a considerable distance might obviate the greater flux at the film edge. Indeed further evidence that the film evaporates over its full extent is seen in the long timescale images where dryout has occurred (especially Figure 4). The gradient of these plots does not appear to vary significantly with morphology.

It was noticed that in some cases after repeated use the film development was less deterministic for FDTS surfaces, so parylene surfaces were also used. For the film to develop in a similar way to ethanol on FDTS coating, a water-ethanol mixture was used, pure water being

too hydrophobic (producing only droplets) and pure ethanol too omniphilic (spreading over the surface as a film only).

In Figure 8, droplet evaporation is seen on plots of mass vs time for 1.5 microlitre droplets of water-ethanol mixture and 4 morphologies (parylene coated surface) and a number of drops. Mass was inferred from goniometric volume. The films formed are once again, largely square (but with imperfect edges). Droplet size variation (which is greater at the small volumes used here) will lead to some scatter in these data, so the plots for all droplets are included. The evaporation rate is fastest for the 5 micron square pillars and proceeds to reduce for greater pillar size.

The movement of the spreading front was also examined to reveal progression, as shown in Figure 9. Film front progression slowed over time, but did not show square root dependence on time.

It is also interesting to note that the mixture film, which loses its more volatile component first, breaks up into water-rich mini-droplets across the film area because of the higher surface tension of the resultant mixture. This is seen in Figure 10, where a distinct mini-droplet has been spawned.

This work paves the way for analogous experiments with nanofluids (currently underway) to study particle deposition in order to elucidate further the mechanisms of heat transfer and fluid flow in these droplets and compare these to “coffee stain” type patterns on flat surfaces. This work should be done either with regularly renewed FDTS surfaces or parylene surfaces. Also, further work on mixture evaporation will be pursued.

CONCLUSIONS

Droplets of ethanol and 50 % ethanol-water mixtures are seen to form films surrounding the droplets as they spread and evaporate on microstructured surfaces. The surface acts to imbibe the fluid and there is a coupled evaporation and fluid-dynamical mechanism to the droplet extent and lifetime. The evaporation rates are faster for droplets with films.

Further work with fluid-particle mixtures will allow deposition patterns on microstructures to be studied.

Acknowledgements

The authors would like to thank MEMStar for the coatings used in this work.

Nomenclature

FDTS	Perflourodecyltrichlorosilane
H_{fc}	Enhalpy, J
l	Front length, mm
m	Mass, g
t	Time, s

REFERENCES

1. Fukutani, Y., Wakui, T., Hussain, S., Kohno, M., Takata, Y., Sefiane, K., and Kim, J., *Effect of Hydrothermal Waves on Evaporation Distribution During Drop Evaporation*, Heat Transfer Engineering, vol 37, no. 7-8, pp. 729-740, 2016.
2. Duursma, G., Kennedy, R., Sefiane, K., and Yu, Y., *Leidenfrost Droplets on*

Microstructured Surfaces, Heat Transfer Engineering vol. 37, no. 13-14, pp. 1190-1200, 2016.

3. Mackenzie-Dover, C., Duursma, G., Christy, J., Terry, J.G., and Sefiane, K., *Effect of micropillar spacing and temperature of substrate on contact angle dynamics,* Heat Transfer Engineering vol. 40, no. 14-15, 2019. DOI:10.1080/01457632.2018.1443246
4. Sefiane, K., Tadrist, L., and Douglas, M., *Experimental study of evaporating water-ethanol mixture sessile drop: influence of concentration*, International journal of heat and mass transfer, vol. 46, no. 23, pp. 4527-4534, 2003.
5. Wasnik, P.S., N'guessan, H.E., and Tadmor, R., *Controlling arbitrary humidity without convection,* Journal of Colloid and Interface Science, vol. 455, pp. 212-219, Oct. 2015.
6. Tadmor, R, Wasnik, P.S., and N'guessam, H.E., *Inducing arbitrary vapor pressures, and quantifying leakages*, AIChEJ, vol. 62, no. 12, pp. 4548-4553, 2016.
7. Papadopoulos. P., Deng, X., Mammen, L., Drotlet, D.-M., Battagliarin, G., Li, C., Mullen, K., Landfester, K., del Campo, A., Butt, H.-J., and Vollmer, D., *Wetting on the microscale: Shape of a Liquid drop on a Microstructured Surface at different Length Scales*, Langmuir, vol. 28, no. 22, pp. 8392-8398, 2012.
8. Chu, K-H., Xiao, R., Wang, E.N., *Uni-directional liquid spreading on asymmetric nanostructured surfaces*, Nature Materials, vol. 9, no. 5, pp. 413-417, 2010.
9. Courbin, L., Denieul, E., Dressaire, E., Roper, M., Ajdari, A., and Stone, H., *Imbibition by polygonal spreading on microdecorated surfaces*, Nature Letters, vol. 6., no. 9, pp. 661 – 664, 2007.
10. Courbin, L., Bird, J.C., Reyssat, M., and Stone, H.A., *Dynamics of wetting: from inertial spreading to viscous imbibition*, Journal of Physics: Condensed Matter, vol. 21, no. 46, pp. 464127:1-13, 2009.

11. Bonn, D., Eggers, J., Indekeu, J., Meunier, J., and Rolley, E., *Wetting and spreading,* Reviews of Modern Physics, vol. 81, no. 2, pp. 739-805, 2009.
12. Hu, H. and Larson, R.G., *Evaporation of a sessile droplet on a substrate*, J. Phys. Chem B, vol. 106, no. 6, pp. 1334-1344, 2002.
13. Tadmor, R., Das, R., Gulec, S., Liu, J., N'guessan, H.E., Shah, M., Wasnik, P.S., and Yadav, S.B., *Solid-Liquid Word of Adhesion*, Langmuir, vol. 33, no. 15, pp. 2594-2600, 2017.
14. Tadmor, R., *Approaches in wetting phenomena*, Soft Matter, vol. 7, no. 5, pp. 1577-1580, 2011.
15. Feng, H., Chong, K.S., Ong, K., and Duan, F., *Octagon to square wetting transition of water-ethanol droplets on a micropyramid substrate by increasing ethanol concentration*, Langmuir, vol. 33, no. 5, pp. 1147-1154, 2017.
16. Zhong, X., Ren, J., Chong, K.S.-L., Ong, K.-S., and Duan, F., *Controlling Octagon-to-square wetting interface transition of evaporating sessile droplet through surfactant on microtextured surface*, Applied Materials and Interfaces, vol. 10, no. 14, pp. 11425-11429, 2018.
17. Tsai, P., Lammertink, R.G.H., Wessling, M., and Lohse, D., *Evaporation triggered wetting transition for water droplets upon hydrophobic microstructures.* Phys. Rev. Letters, vol. 104, no. 11, pp. 116102:1-4, 2010.
18. Tadmor, R., Bahadur, P., Leh, A., N'guessan, H.E., Jaini, R., and Dang, L., *Measurement of Lateral Adhesion Forces at the Interface between a Liquid Drop and a Substrate*, Physical Review Letters, vol. 103, no. 26, pp. 266101:1-4, 2009.
19. N'guessan, H.E., Leh, A., Cox, P., Bahadur, P., Tadmor, R., Patra, P., Vajtai, R., Ajayan,

P.M., and Wasnok, P., *Water tribology on graphene*, Nature Communications, vol. 3, no.1, pp. 1242:1-5, 2012.

Table 1 Evaporation as mass and enthalpy rates

	Pillar Size	5 μm	10 μm	20 μm	40 μm
Evaporation Mass Rate:	$\frac{dm}{dt}(g/s)$	8.95×10^{-6}	7.00×10^{-6}	7.00×10^{-6}	8.31×10^{-6}
Evaporative Heat Rate:	$\frac{dH_{fc}}{dt}(J/s)$	0.0139	0.0108	0.0108	0.0129

List of figure captions

Figure 1 Schematic diagram of experimental facility and close up of the surface and syringe

Figure 2 Four microlitre droplet shapes when deposited on various substructures

Figure 3 Film evaporation of 4 microlitre droplets in time on a 5 x 5 micron 5 micron spacing surface (a-c); with 10 micron spacing (d-f); with 10 x 10 micron pillars (g-i); and with all dimensions 10 microns (j-l).

Figure 4 Droplet evaporation showing the film persistence

Figure 5 Film spreading and evaporation (4 microlitre droplet)

Figure 6 Evaporation rate (volume vs time) for droplet with films and without for 10 micron cylindrical pillars at various spacings

Figure 7 Change of droplet height with time for three different droplets

Figure 8 Graph of mass vs time for droplets on 4 different morphologies

Figure 9 Development of the film front

Figure 10 Mini-droplet formation in the film as the mvc evaporates

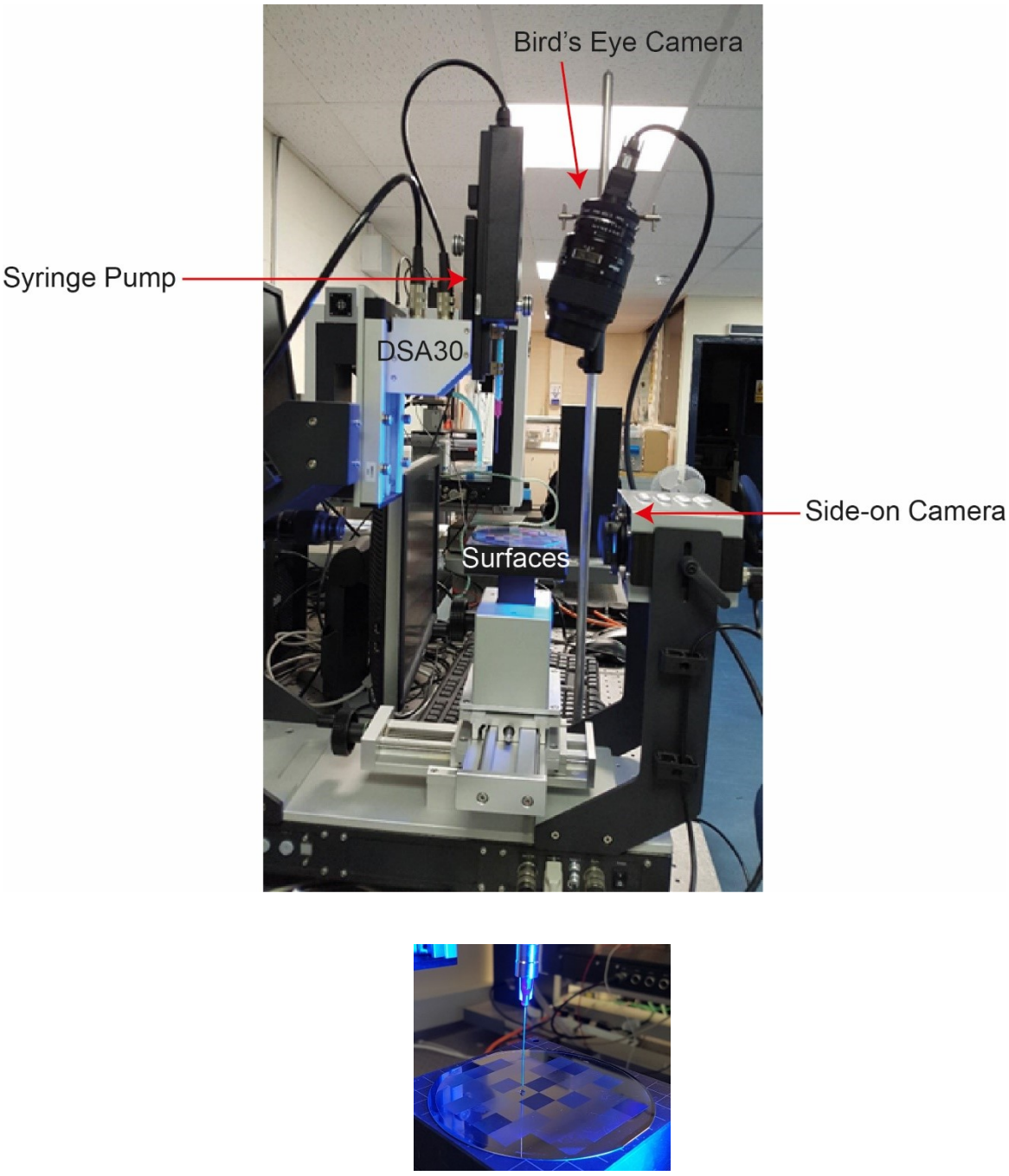

Fig. 1 Schematic diagram of experimental facility and close up of the surface and syringe

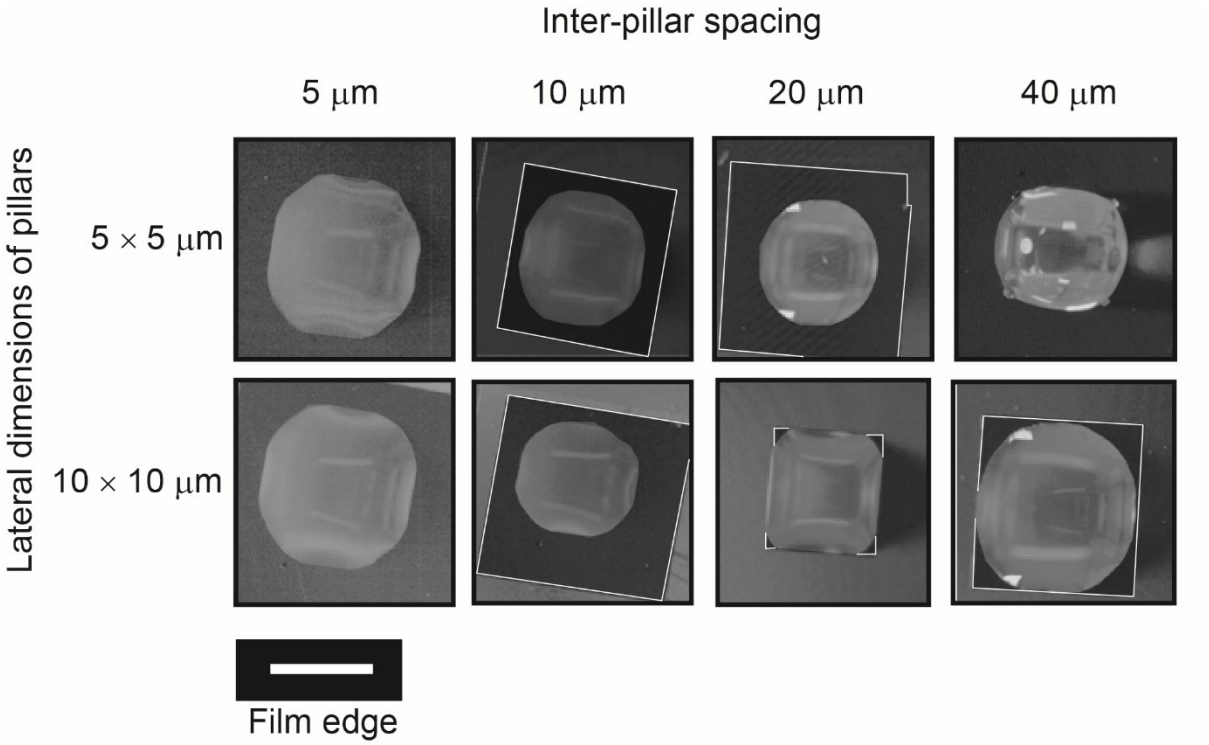

Fig 2 Four microlitre droplet shapes when deposited on various substructures

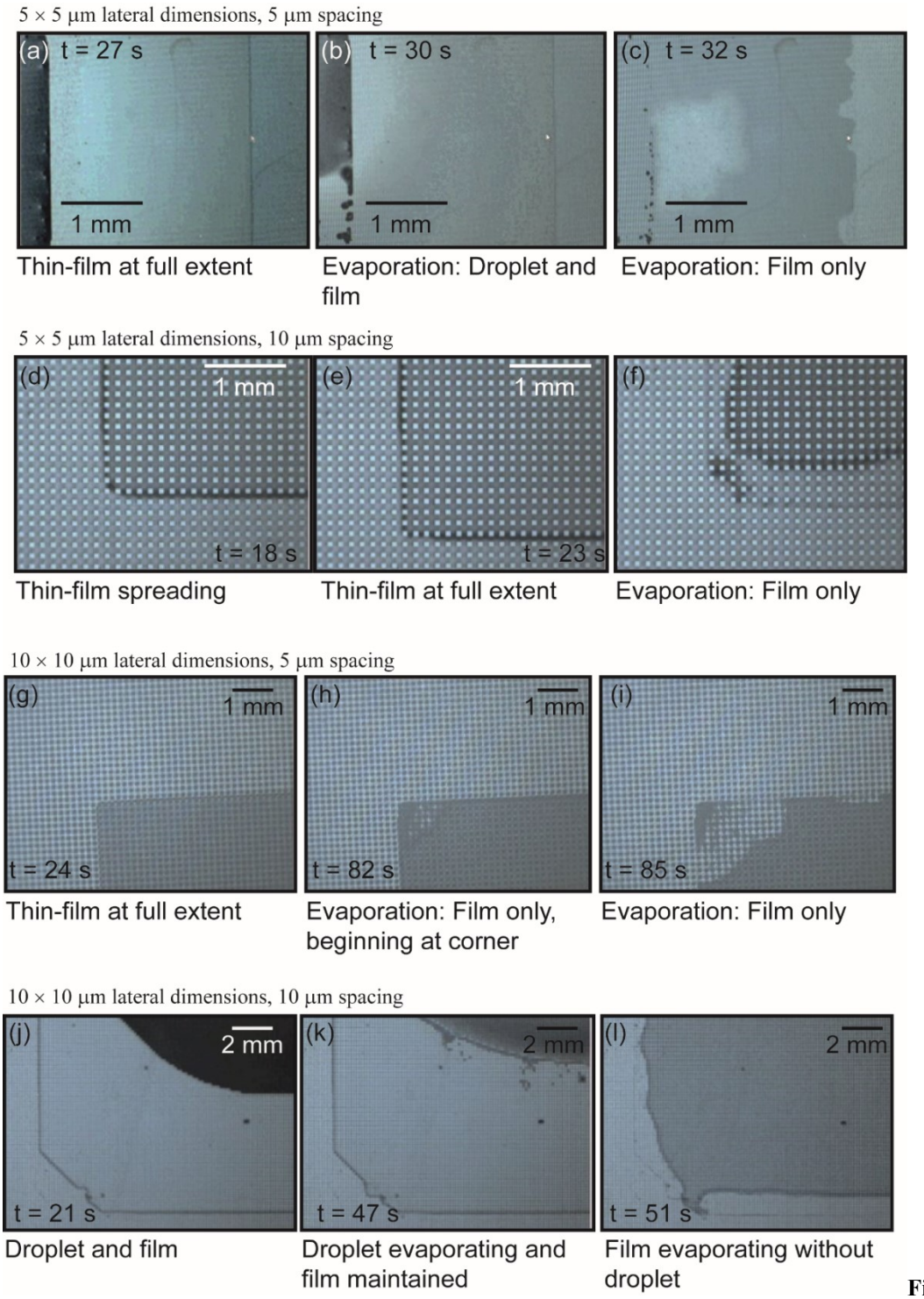

Fig 3 Film evaporation of 4 microlitre droplets in time on a 5 x 5 micron 5 micron spacing surface (a-c); with 10 micron spacing (d-f); with 10 x 10 micron pillars (g-i); and with all dimensions 10 microns (j-l).

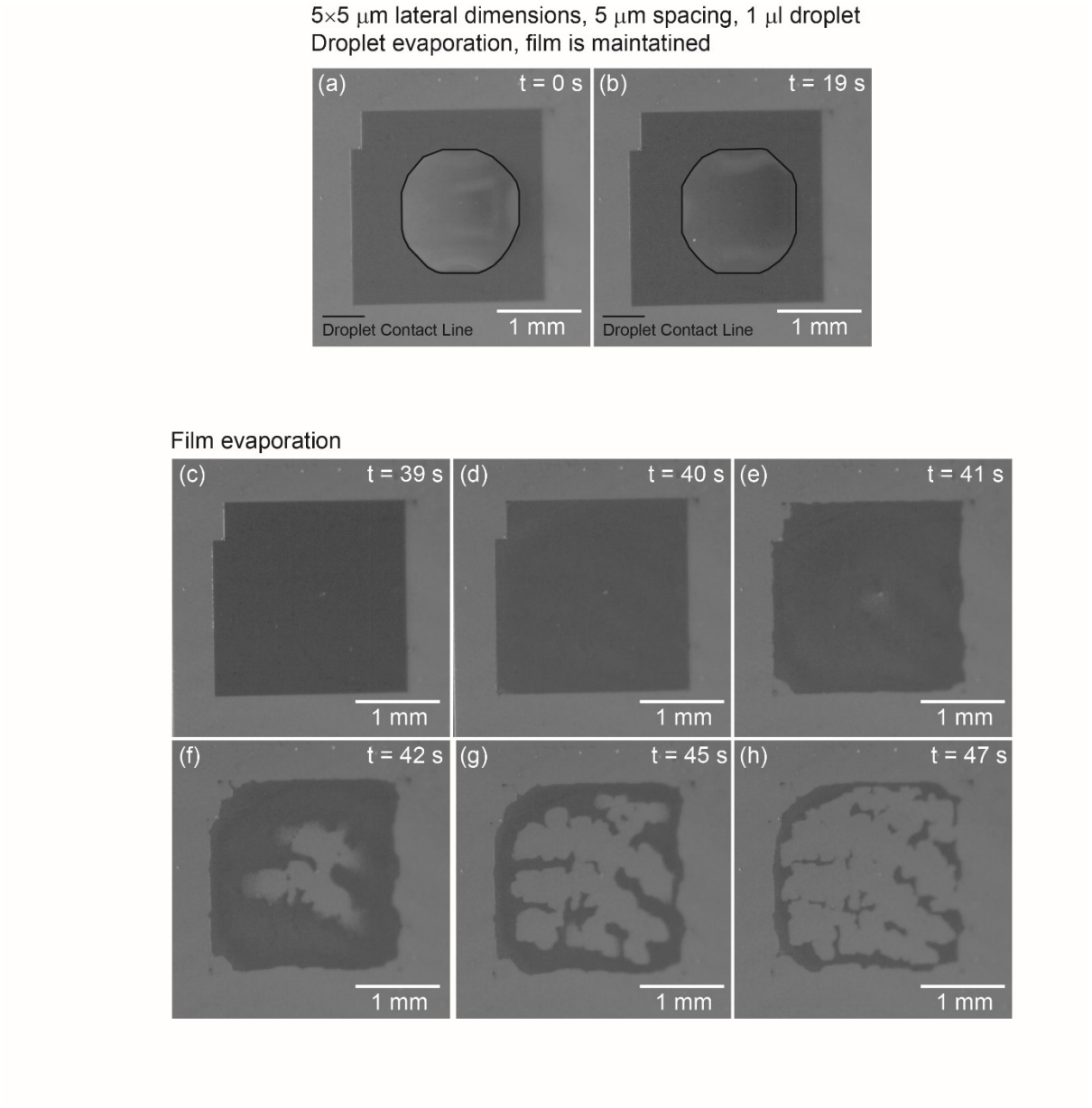

Figure 4 Droplet evaporation showing the film persistence

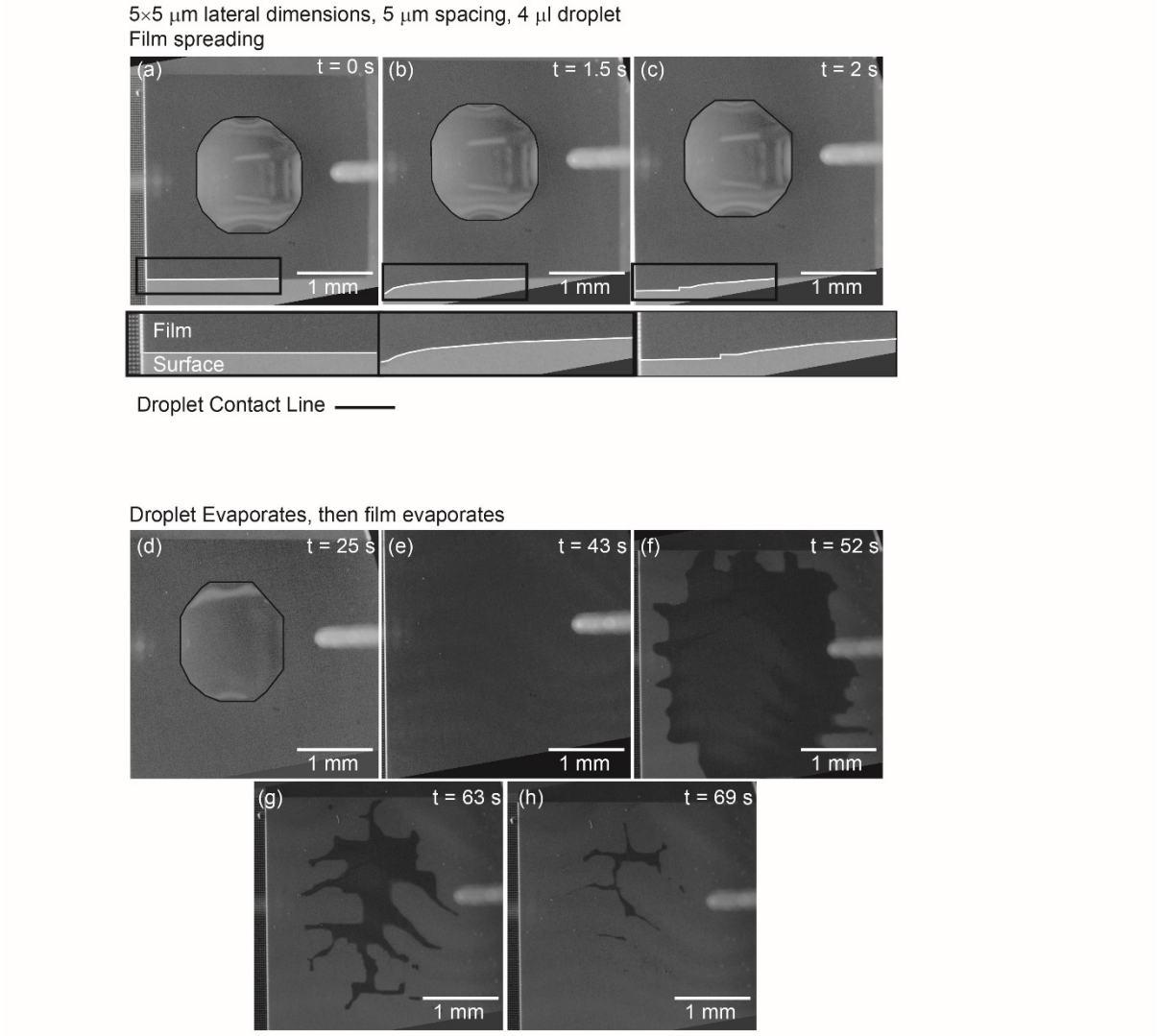

Figure 5 Film spreading and evaporation (4 microlitre droplet)

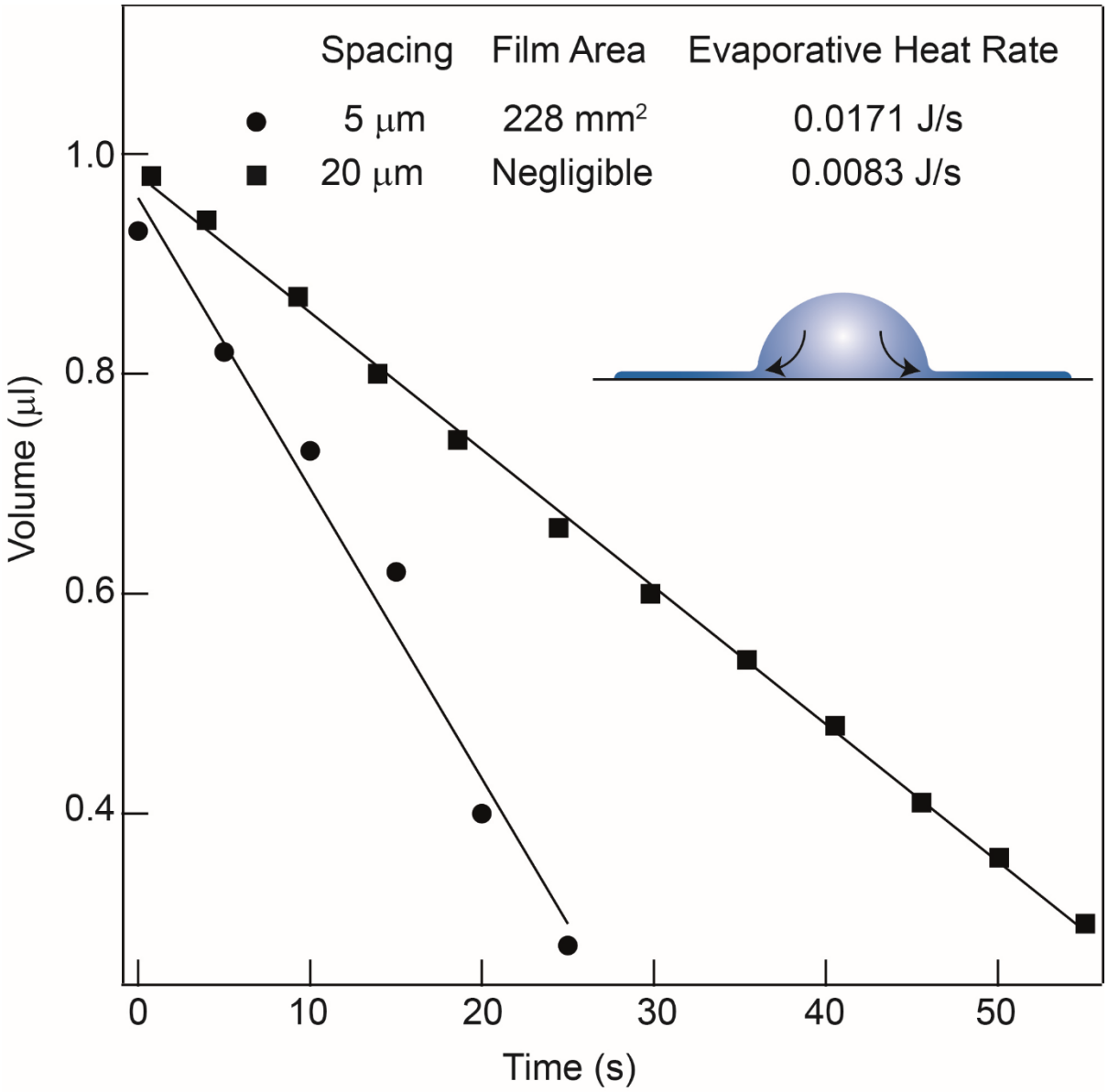

Figure 6 Evaporation rate (volume vs time) for droplet with films and without for 10 micron cylindrical pillars at various spacings

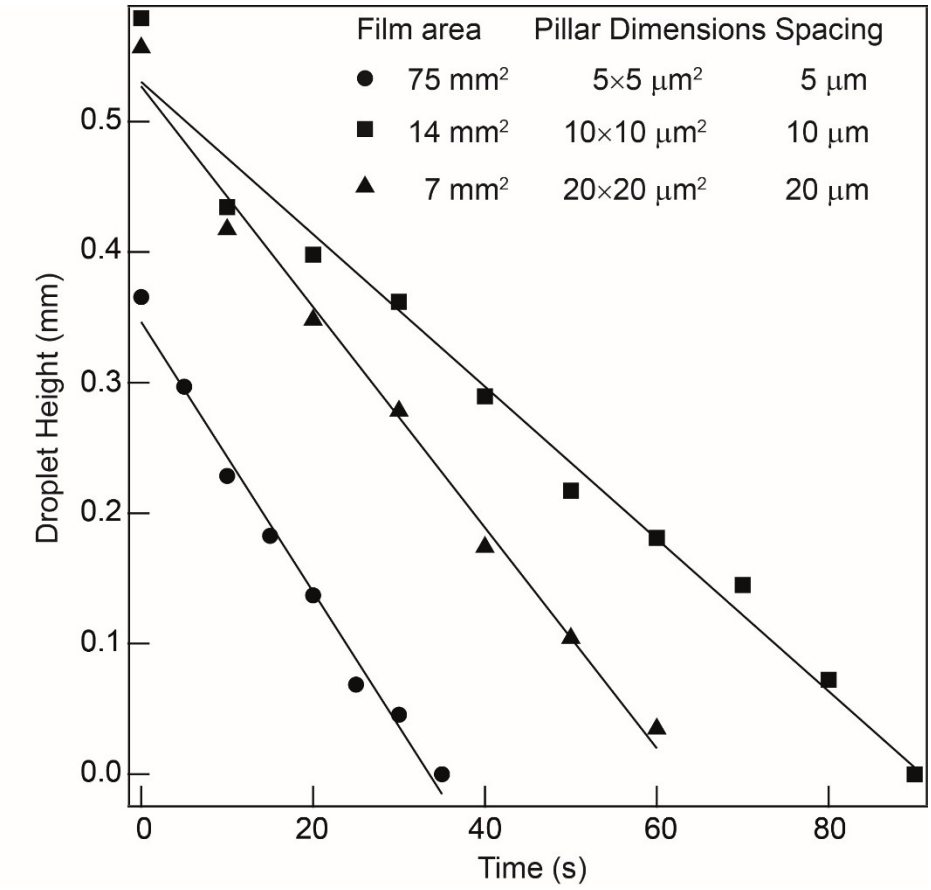

Figure 7 Change of droplet height with time for three different droplets.

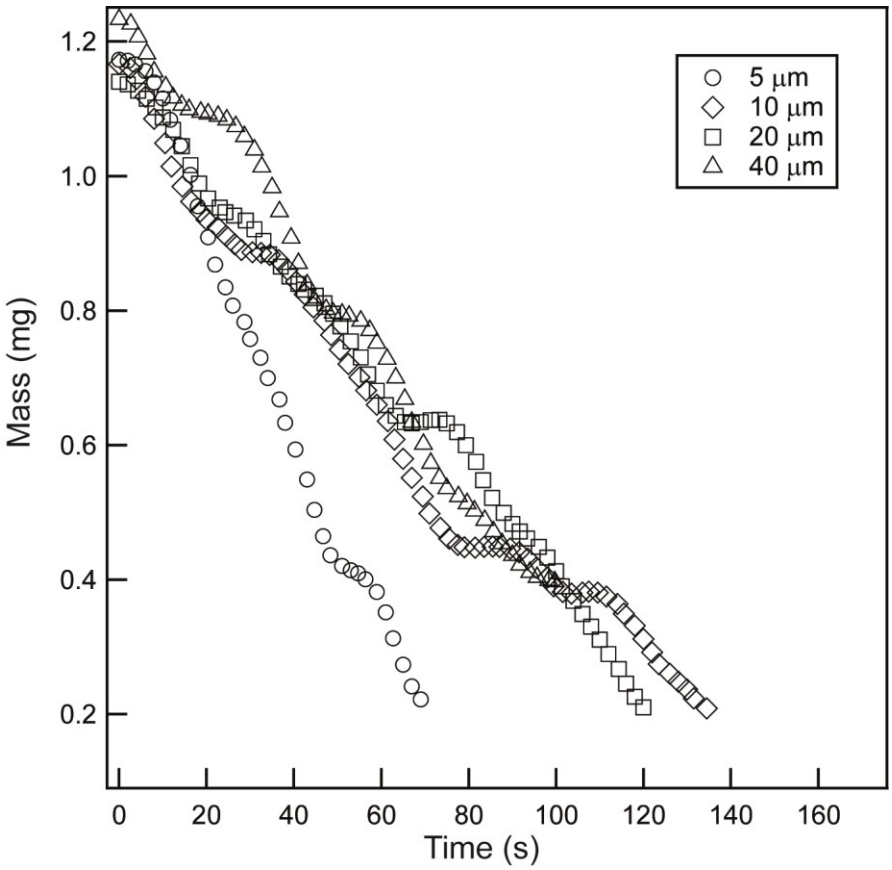

Figure 8 Graph of mass vs time for droplets on 4 different morphologies

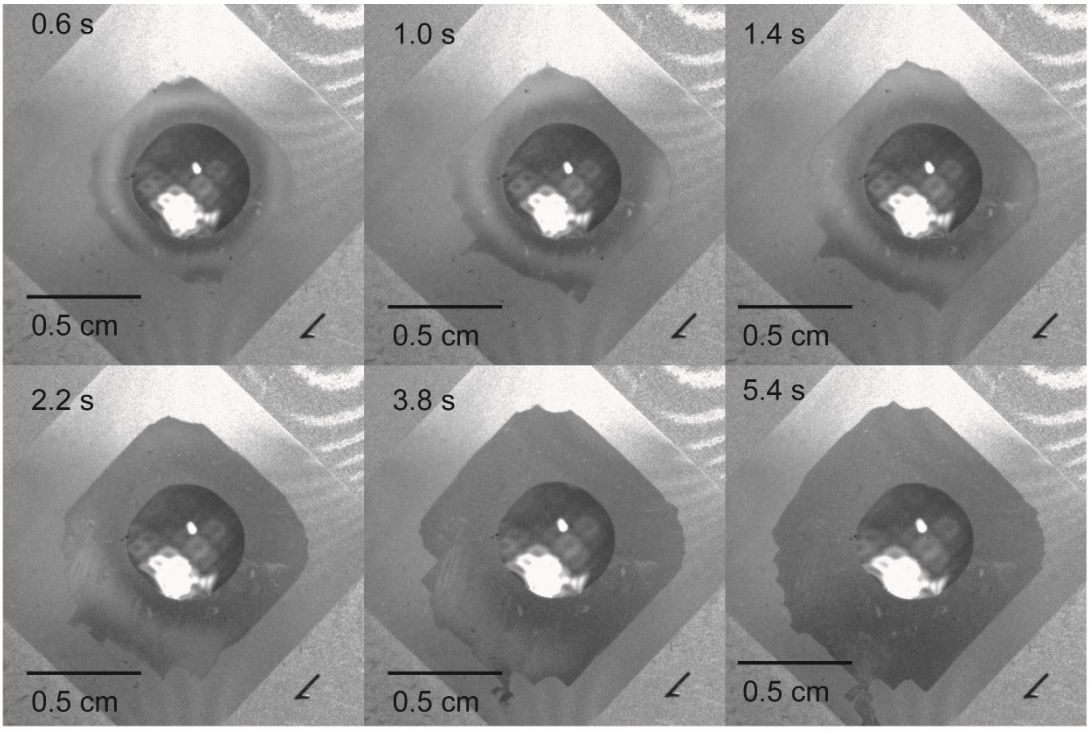
0.6 s
0.5 cm
1.0 s
0.5 cm
1.4 s
0.5 cm
2.2 s
0.5 cm
3.8 s
0.5 cm
5.4 s
0.5 cm

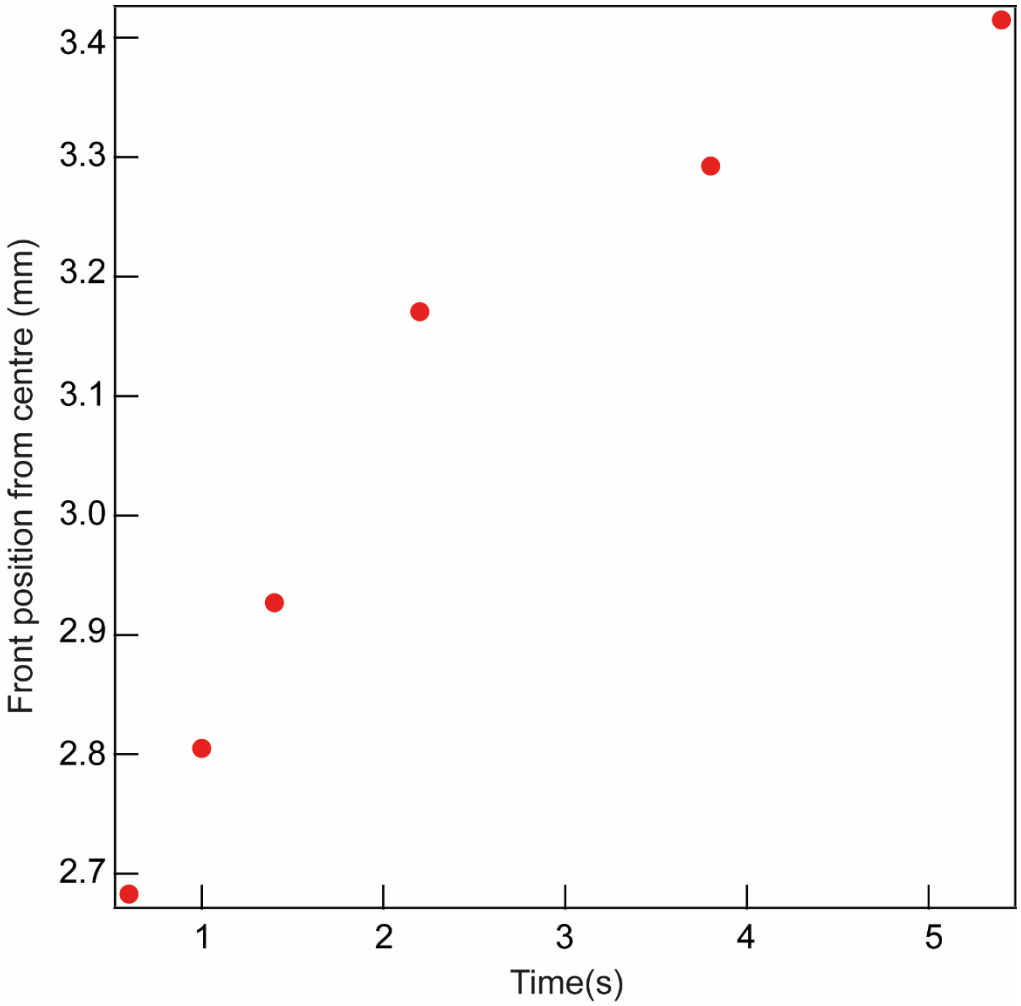

Figure 9 Development of the film front

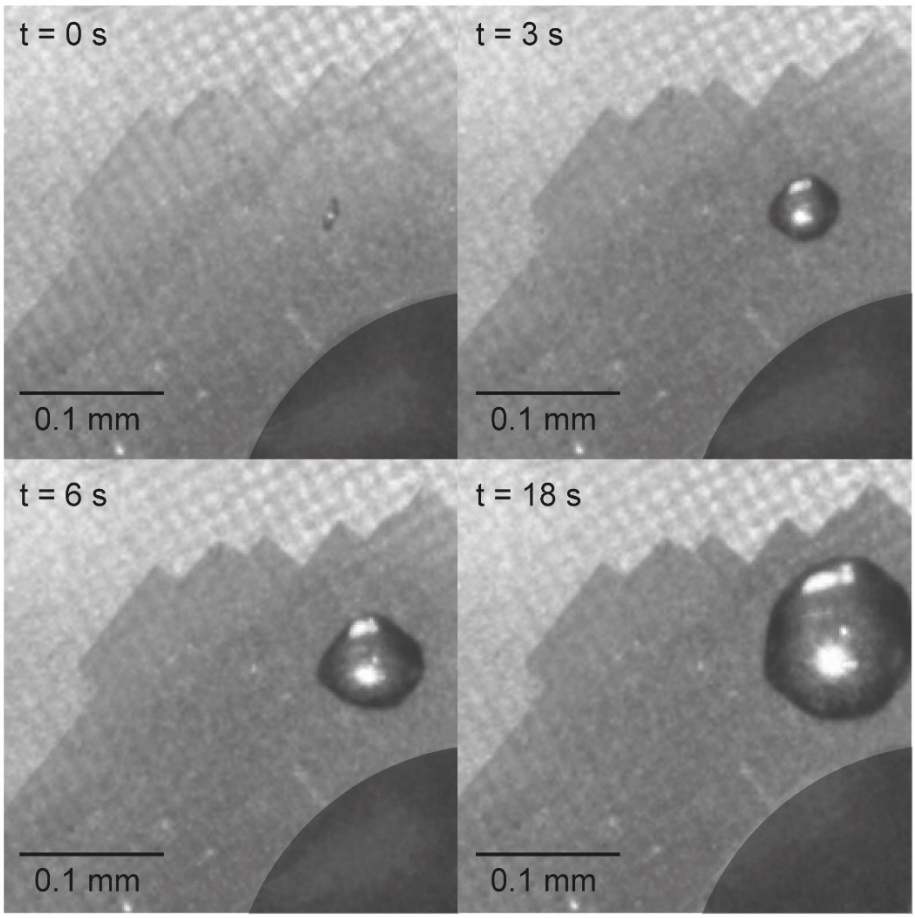

Figure 10 Droplet spawning from the film

Biographical details

Revekka Tekidou is an MSc research student at the University of Edinburgh in the Institute of Multiscale Thermofluids. She is a graduate of the Aristotle University of Thessaloniki.

Gail Duursma is a Senior Lecturer in Chemical Engineering at the University of Edinburgh. She obtained her D.Phil. from the University of Oxford and after post-doctoral study at the University of Oxford, she joined the University of Edinburgh. She is a Member of the IChemE.

Coinneach Mackenzie-Dover is a Reseaarch Associate at the University of Edinburgh (Institute for Integrated Micro and Nano Systems). He has a PhD in Condensed Matter Physics subsequent to undergraduate studies at the University of Edinburgh. He is currently undertaking work examining the relationship between surface structure and wettability.

Veronika Kubyshkina is a PhD student at the University of Edinburgh in the Institute of Multiscale Thermofluids. She graduated with an MEng in Chemical Engineering in 2017 from the University of Edinburgh.

Jonathan Terry is a Chancellor's Fellow and Lecturer in the School of Engineering at University of Edinburgh for over fifteen years primarily researching the development of more-than-Moore technologies, the integration of novel fabrication processes and materials with foundry CMOS to create smart sensors and microsystems.

Khellil Sefiane has MSc and PhD degrees in Chemical Engineering. He presently holds the Chair of Thermophysical Engineering at the University of Edinburgh. He is also ExxonMobil Fellow at the University of Edinburgh.